Characterizing Touch Using Pressure Data and Auto Regressive Models

Shlomi Laufer, *Member, IEEE,* Carla M. Pugh, Barry D. Van Veen, *Fellow, IEEE*

***Abstract*— Palpation plays a critical role in medical physical exams. Despite the wide range of exams, there are several reproducible and subconscious sets of maneuvers that are common to examination by palpation. Previous studies by our group demonstrated the use of manikins and pressure sensors for measuring and quantifying how physicians palpate during different physical exams. In this study we develop mathematical models that describe some of these common maneuvers. Dynamic pressure data was measured using a simplified testbed and different autoregressive models were used to describe the motion of interest. The frequency, direction and type of motion used were identified from the models. We believe these models can a provide better understanding of how humans explore objects in general and more specifically give insights to understand medical physical exams.**

I. INTRODUCTION

Palpation plays a critical role in many medical physical exams, such as the clinical breast exam (CBE), digital rectal exam (DRE) and the pelvic exam [1]–[3]. Extensive research done by Klatsky and Lederman showed that when humans explore objects they use a reproducible and subconscious set of maneuvers, named exploratory procedures (EPs) [4], [5]. In their studies they established links between the hand movement and the desired knowledge acquired. The EPs and their associated object properties are: lateral motion (texture), pressure (hardness), static contact (temperature), unsupported holding (weight), enclosure (global shape) and contour following (global shape). While their studies focused on general object exploration, these EPs can be used for analyzing and understanding physical exams.

In our previous studies we used sensor-enabled medical simulators in order to capture and quantify human palpation during physical exams [6]–[8]. We were able to measure and categorize different techniques used during these physical exams [9], [10]. In this study we focus on the more basic and fundamental work of developing mathematical models of the EPs based on pressure data. More specifically, we develop multi-variable auto regressive (MVAR) models of lateral motion and pressure EPs, which play a critical role in many clinical exams. The data for this current study was collected using a simplified testbed and palpation maneuvers associated with those known to be typical of the CBE.

Current recommendations for the CBE suggest using circular motions when performing the exam [1]. In addition when a suspicious mass is found its stiffness is typically assed by applying pressure. Therefore, in this project we focus on lateral motion and pressure. This approach is in accordance with our previous studies which showed that two of the most fundamental maneuvers commonly used by medical examiners were rubbing (lateral motion) and tapping (pressure) [10]. In this manuscript we divided the rubbing to two groups: circular rubbing and linear rubbing. We believe the former is recommended for the CBE and the latter is common to regular texture recognition.

In the next section the mathematical models for the different EPs will be presented. This will be followed by the description of the data collected and the experiment performed. Then the results will be presented and the suggested approach will be discussed.

II. METHODS

A. MVAR Model

In this study three 2-dimensional MVAR models for motion in the $x-y$, $x-z$ and $y-z$ planes were calculated.

A 2-dimensional MVAR model of order p is described by the following equation:

$$\mathbf{u}_n = \sum_{l=1}^{p} \mathbf{A}_l \mathbf{u}_{n-l} + \boldsymbol{\varepsilon}_n \tag{1}$$

where $\mathbf{u}_n$ is a 2×1 time series vector at time index n representing the two components of motion being modeled, $\boldsymbol{\varepsilon}_n$ is the noise at time index n and $\mathbf{A}_l$ are the 2×2 MVAR parameter matrices. It is assumed the data is zero mean, an assumption that can be met by subtracting the mean of the data from the measured data. A $p=1$ order model was used for circular rubbing while a $p=2$ order model was used for linear rubbing. Without loss of generality we will assume that the rubbing motion occurs in the $x-y$ plane.

B. Circular rubbing: model order $=1$

One iterative method to draw a circle is using a circle generating matrix [11], [12]. Given one point on the radius of the circle, $[x_0, y_0]$ and a step size h a circle can be drawn using the next iterative algorithm:

$$\begin{bmatrix} x_n \\ y_n \end{bmatrix} = \begin{bmatrix} \cos(h) & -\sin(h) \\ \sin(h) & \cos(h) \end{bmatrix} \cdot \begin{bmatrix} x_{n-1} \\ y_{n-1} \end{bmatrix} \tag{2}$$

The origin of the circle will be at $[0,0]$ and the radius will be $\sqrt{x_0^2+y_0^2}$. In addition h governs the distance between

This work was supported by the National Institutes of Health R01EB011524 Grant titled Validation of Sensorized Breast Models for High Stakes Testing.

S. Laufer is with the Department of Surgery and with the Department of Electrical and Computer Engineering, University of Wisconsin-Madison, Madison, WI 53706 USA (e-mail: slaufer2@wisc.edu)

C.M. Pugh is with the Department of Surgery, University of Wisconsin-Madison ,Madison, WI 53706 USA (e-mail: pugh@surgery.edu)

B.D. Van Veen is with the Department of Electrical and Computer Engineering, University of Wisconsin-Madison, Madison, WI 53706 USA (e-mail: vanveen@engr.wisc.edu)

978-1-4244-7929-0/14/$26.00 ©2014 IEEE

adjacent points and $N = \frac{2\pi}{h}$ points will be required for a complete circle. Since a $p = 1$ order model in the $x-y$ plane is given by

$$\begin{bmatrix} x_n \\ y_n \end{bmatrix} = \mathbf{A}_1 \cdot \begin{bmatrix} x_{n-1} \\ y_{n-1} \end{bmatrix} + \varepsilon_n \tag{3}$$

then (2) implies that circular rubbing is described by

$$\mathbf{A}_1 = \begin{bmatrix} \cos(h) & -\sin(h) \\ \sin(h) & \cos(h) \end{bmatrix} \tag{4}$$

where the rubbing frequency f_0 is

$$f_0 = \frac{h \cdot f_s}{2\pi} \tag{5}$$

and f_s is the sampling frequency. In the more general case of an elliptic movement, the iterative generating matrix is

$$\mathbf{A}_1 = \begin{bmatrix} \cos(h) + \sin(h)\sin(\theta)\cos(\theta) \cdot (\alpha - 1/\alpha) & -\sin(h) \cdot (\sin^2(\theta)/\alpha + \cos^2(\theta) \cdot \alpha) \\ \sin(h) \cdot (\cos^2(\theta)/\alpha + \sin^2(\theta) \cdot \alpha) & \cos(h)) - \sin(h)\sin(\theta)\cos(\theta) \cdot (\alpha - 1/\alpha) \end{bmatrix} \tag{6}$$

where θ is the rotation of the ellipse and α is the ratio of the major and minor axis. The unknown parameters can be extracted according to

$$\mathbf{A}_1 \triangleq \begin{bmatrix} a_{1,1} & a_{1,2} \\ a_{2,1} & a_{2,2} \end{bmatrix} \tag{7}$$

$$h = \cos^{-1}\left(\frac{a_{1,1} + a_{2,2}}{2}\right) \tag{8}$$

$$\theta = \frac{1}{2}\tan^{-1}\left(\frac{a_{2,2} - a_{1,1}}{a_{2,1} + a_{1,2}}\right) \tag{9}$$

$$\alpha = \frac{1}{2}\left[\frac{a_{2,1} - a_{1,2}}{\sin(h)} + \sqrt{\left(\frac{a_{2,1} - a_{1,2}}{\sin(h)}\right)^2 - 4}\right] \tag{10}$$

C. Linear rubbing: model order = 2

We start with a simple canonical form of linear motion where the rubbing is described as a sinusoidal variation in the x direction. That is

$$x_n = sin(2\pi f_0 n / f_s) \tag{11}$$

where f_0 is the frequency of the rubbing in Hz and f_s is the sampling frequency.

In a similar manner to the circular motion, an iterative sinusoidal motion generating function is defined as

$$x_n = a_1 x_{n-1} + a_2 x_{n-2} \tag{12}$$

where the amplitude and phase of the sine is determined by the initial conditions x_0 and x_1 . The coefficients a_1 and a_2 control the step size and are given by $a_1 = 2\cos(h)$ and $a_2 = -1$. As before $N = \frac{2\pi}{h}$ points are needed to finish one cycle so $f_0 = h \cdot f_s / 2\pi$ expresses the rubbing frequency as a function of the step size.

Rotation of (12) to linear rubbing at an angle θ with respect to the x-axis gives the $p = 2$ order model in the $x-y$ plane

$$\begin{bmatrix} x_n \\ y_n \end{bmatrix} = \mathbf{A}_1 \cdot \begin{bmatrix} x_{n-1} \\ y_{n-1} \end{bmatrix} + \mathbf{A}_2 \cdot \begin{bmatrix} x_{n-2} \\ y_{n-2} \end{bmatrix} + \varepsilon_n \tag{13}$$

where

$$\mathbf{A}_1 = \mathbf{R}^{-1}\begin{bmatrix} a_1 & 0 \\ 0 & 0 \end{bmatrix}\mathbf{R}, \quad \mathbf{A}_2 = \mathbf{R}^{-1}\begin{bmatrix} a_2 & 0 \\ 0 & 0 \end{bmatrix}\mathbf{R} \tag{14}$$

and $\mathbf{R}$ is the rotation matrix

$$\mathbf{R} = \begin{bmatrix} \cos(\theta) & -\sin(\theta) \\ \sin(\theta) & \cos(\theta) \end{bmatrix} \tag{15}$$

Note that (14) expresses both $\mathbf{A}_1$ and $\mathbf{A}_2$ as the product of a matrix with orthonormal columns, a diagonal matrix, and the transpose of the first matrix. Therefore, we can regard these expressions as eigendecompositions of the matrices $\mathbf{A}_1$ and $\mathbf{A}_2$. The eigenvectors define the rotation angle θ and the eigenvalues the rubbing frequency f_0. Once we estimate the entries of the matrices $\mathbf{A}_1$ and $\mathbf{A}_2$ from the data, we use eigendecomposition to identify the rotation angle and rubbing frequency.

Due to noise in the estimated $\mathbf{A}_1$ and $\mathbf{A}_2$, the eigenvectors of each matrix may differ and not form a rotation matrix, and there may be two nonzero eigenvalues. We estimate the angle using the eigenvector associated with the largest eigenvalue.

D. Error Calculation and Model Selection

Both MVAR models were calculated for all test maneuvers and the model with the minimum error was chosen as best representing the motion. The error for each model was calculated in the following way

- $p = 1$ - A dense ellipse was generated using the model parameters and a measured data point. This was done using the ellipse generating matrix and decreasing the step size h by a factor of 10. For every measured data point the error was given as the distance of the point to the closest point on the dense ellipse.
- $p = 2$ - The error was calculated as the distance of the measured data from the line equation produced by the model .

Due to the symmetric nature of the inverse of harmonic functions (e.g. $\cos^{-1}$) there is ambiguity regarding the angle of the model. For ellipsoidal motion the angle is either θ or $\theta + \pi/4$ and for linear motion the angle is either θ or $\theta + \pi/2$. Therefore, errors for both angle options were checked. For a given motion the model chosen was the one that minimized the square error. Note that since the motion was symmetric around the origin there is no difference between θ and $\theta + \pi$ and therefore θ was constrained to $0 \leq \theta < \pi$.

E. Exploratory procedures selection

While rubbing can be modeled as a line or a circle in the $x-y$ plane, tapping typically involves linear motion in the $x-z$ and $y-z$ planes. For example canonic rubbing is described by $x_n = \sin(2\pi f_0 n / f_s)$, $y_n = 0$ and $z_n = 0$

while canonic tapping is described by $x_n = 0$, $y_n = 0$ and $z_n = \sin(2\pi f_0 n/f_s)$. Therefore tapping and rubbing can be differentiated by analyzing the angle given by a model in the $x-z$ plane. Thus for each motion, models in all three planes were calculated. If the angle in both $x-z$ and $y-z$ was above 80° then taping was selected, otherwise rubbing. Note that if there is no motion in two axes, for example y and z in the canonic rubbing, then the matching model ($y-z$) will be noisy and meaningless. Therefore both models had to satisfy this criteria for the motion to be tapping.

The MVAR model for each sample was computed by minimizing the squared error over the preceding 30 samples. Then each sample was categorized as tapping, circular rubbing or linear rubbing based on the error analysis described in the previous section. A majority vote was used to declare which procedure was associated with each exploration.

III. DATA

A. Participants

Four participants (2 male 2 female, average age 32) gave informed consent to the protocol approved by the University of Madison Institutional Review Board.

B. Testbed preparation and apparatus

The testbed was constructed from a two-component rubber silicon (Ecoflex®0030, Smooth-On Inc., Shore 00-30 hardness) mixed in a 1:1 ratio . The same family of materials is used in our breast simulators [8]. The testbed was a 200x200 mm flat surface, 8 mm thick, placed on a pressure mapping system (Fig. 1). The pressure mapping system included a 250 x 250 mm ultra-thin, tactile pressure sensor, comprised of 1,936 individual sensing elements uniformly distributed in a 44 x 44 matrix (Tekscan®Boston, MA). The sensor map was connected to the computer's USB using a designated data acquisition handle. Data were sampled at 90 Hz and stored for offline analysis. In addition video recordings of hand movement were acquired.

C. Preprocessing of pressure data

The pressure data were transformed to the finger location in space before modeling the data. Using a right handed coordinate system, let the z direction be the normal to the testbed. The $x-y$ position of the finger was calculated based on the center of force. First the pressure map was up-sampled by a factor of 5 using the nearest neighbor algorithm, resulting in a 220×220 image. The image was filtered using a 17×17 Gaussian filter and the pixel with the maximum value was taken as the center of force.

The actual displacement in the z direction depends on the physical properties of the testbed. In thick and soft testbeds larger displacements will be measured for the same amount of force applied. Nevertheless, for modeling the type of motion, the force applied is more important than the actual displacement of the finger. Therefore force was treated as virtual motion in the z direction. The measured force was divided by an empirical constant which caused the z direction virtual motion to be in the same order of magnitude as the $x-y$ direction motion.

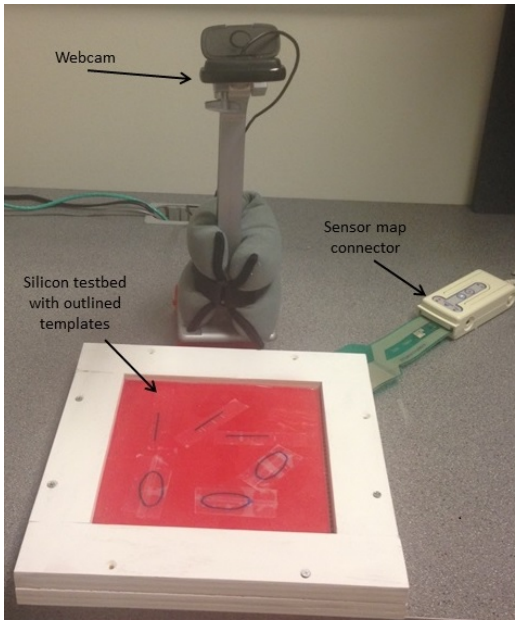

Fig. 1. Silicon based testbed with camera and sensor map, showing the templates used to guide motion.

Since initial analysis showed that on average the palpation frequency was less then 3 Hz, data were down-sampled to 10 Hz before modeling.

D. Experiment

Participants were asked to explore by rubbing and tapping the testbed. An outline for the rubbing pattern was depicted on the testbed in order to allow quantification of the rubbing exploration. Three lines were drawn at angles 0°, 45° and 90°. In addition three ellipses were drawn with major axes in the same directions. The lines were 4 cm long and the major and minor axes of the ellipses were 2 and 4 cm long, respectively (Fig. 1).Tapping was performed in an arbitrary location on the testbed. For each exploration participants were instructed to go back and forth between 5-15 times over the outlined shape trying to keep a constant frequency. Each pattern was explored twice and participants were asked to perform one exploration in what they consider a comfortably slow manner and one in a comfortably fast manner, so a range of frequencies can be measured.

IV. RESULTS

A total of 8 tapping explorations, 24 linear rubbing explorations and 24 circular rubbing explorations were performed. They included 446,1746 and 2184 data points respectively. On average 97% of tapping data points , 99% of linear rubbing data points and 94% of circular rubbing data points were correctly classified. All explorations were correctly classified based on the most frequent data point type in that exploration. A plot of the rubbing direction estimation is shown in Fig. 2. Video data was utilized to validate frequency estimation by counting the number of back and forth

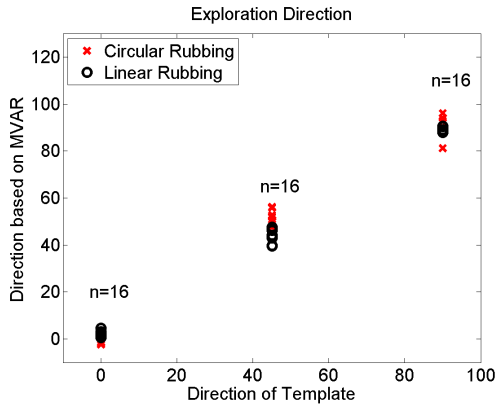

Fig. 2. The exploration direction estimated by the model as a function of the template direction.

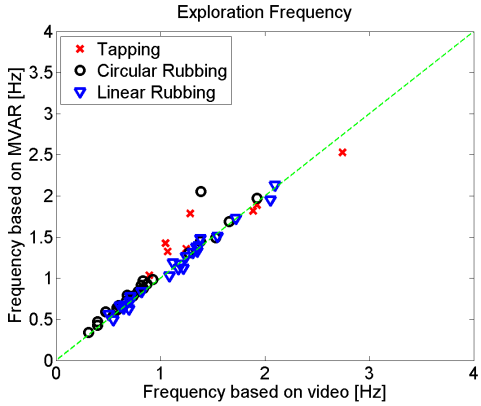

Fig. 3. The exploration frequency estimated by the model depicted as a function of the frequency based on video analysis.

movements and the time they took. An average frequency was calculated from the ratio. This was compared to the average frequency extracted from the models (Fig. 3). The average value of the ellipse axes ratio α was 0.52 ± 0.045; the individual estimated values are depicted in Fig 4.

V. DISCUSSION

In this study several basic maneuvers used for manually exploring objects were modeled using MVAR models. Two fundamental models of linear motion and circular motion were developed. Differentiating between linear rubbing, circular rubbing and tapping was demonstrated by applying them in different coordinate planes. Very good classification was achieved both of the overall exploration and of the exploration for each data point. The models inherently provide information such as palpation frequency and direction in addition to automatic classification of exploratory maneuvers.

We evaluated the accuracy and usefulness of these models using constrained motion. Once established, these models can be used for general motion, and provide insight to how people explore objects. Besides the general interest in human touch, this information is valuable for understanding and potentially improving different medical physical exams. Questions such as palpation technique, direction and frequency can be resolved using these models. In addition comparison between the palpation technique of the general population and of medical experts can be performed. Since a new model is fit to each new time sample, this approach can also be used to characterize more complex motions and dynamically follow transitions between different EPs and multiple rubbing directions.

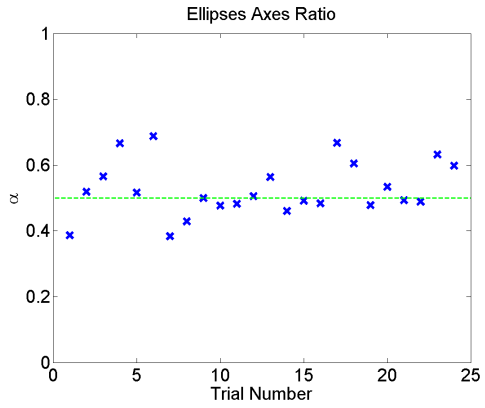

Fig. 4. Model estimated ellipse axis ratio.

REFERENCES

[1] D. Saslow, J. Hannan, J. Osuch, M. H. Alciati, C. Baines, M. Barton, J. K. Bobo, C. Coleman, M. Dolan, G. Gaumer, D. Kopans, S. Kutner, D. S. Lane, H. Lawson, H. Meissner, C. Moorman, H. Pennypacker, P. Pierce, E. Sciandra, R. Smith, and R. Coates, "Clinical breast examination: practical recommendations for optimizing performance and reporting," *CA Cancer J Clin*, vol. 54, no. 6, pp. 327–44, 2004.

[2] N. J. Talley, "How to do and interpret a rectal examination in gastroenterology," *The American journal of gastroenterology*, vol. 103, no. 4, p. 820, 2008.

[3] N. J. Talley and S. O'Connor, *Clinical examination: a systematic guide to physical diagnosis*. Elsevier Australia, 2010.

[4] R. L. Klatzky and S. J. Lederman, "Stages of manual exploration in haptic object identification," *Percept Psychophys*, vol. 52, no. 6, pp. 661–70, 1992.

[5] S. J. Lederman and R. L. Klatzky, "Hand movements: a window into haptic object recognition," *Cogn Psychol*, vol. 19, no. 3, pp. 342–68, 1987.

[6] R. Balkissoon, K. Blossfield, L. Salud, D. Ford, and C. Pugh, "Lost in translation: unfolding medical students' misconceptions of how to perform a clinical digital rectal examination," *The American Journal of Surgery*, vol. 197, no. 4, pp. 525–532, 2009.

[7] C. M. Pugh, S. Srivastava, R. Shavelson, D. Walker, T. Cotner, B. Scarloss, M. Kuo, C. Rawn, P. Dev, T. H. Krummel, and L. H. Heinrichs, "The effect of simulator use on learning and self-assessment: the case of stanford university's e-pelvis simulator," *Stud Health Technol Inform*, vol. 81, pp. 396–400, 2001.

[8] C. M. Pugh, Z. B. Domont, L. H. Salud, and K. M. Blossfield, "A simulation-based assessment of clinical breast examination technique: do patient and clinician factors affect clinician approach?" *The American Journal of Surgery*, vol. 195, no. 6, pp. 874–880, 2008.

[9] S. Laufer, E. R. Cohen, A.-L. Maag, C. Kwan, B. VanVeen, and C. M. Pugh, "Multimodality approach to classifying hand utilization for the clinical breast examination," *Medicine Meets Virtual Reality 21: NextMed/MMVR21*, vol. 196, p. 238, 2014.

[10] L. H. Salud and C. M. Pugh, "Use of sensor technology to explore the science of touch," *Studies in health technology and informatics*, vol. 163, p. 542, 2011.

[11] C. B. Moler, *Numerical computing with MATLAB*. Siam, 2008.

[12] L. Smith, "Drawing ellipses, hyperbolas or parabolas with a fixed number of points and maximum inscribed area," *The Computer Journal*, vol. 14, no. 1, pp. 81–86, 1971.